PHYSICAL REVIEW B **83**, 041302(R) (2011)

One-dimensional ZnO exciton polaritons with negligible thermal broadening at room temperature

A. Trichet,[1] L. Sun,[2] G. Pavlovic,[3] N.A. Gippius,[3,4] G. Malpuech,[3] W. Xie,[2] Z. Chen,[2] M. Richard,[1] and Le Si Dang[1]

[1]*Institut Néel, CNRS, Commissariat à l'Energie Atomique and Université Joseph Fourier, BP 166, F-38042 Grenoble Cedex 9, France*

[2]*Surface Physics Laboratory, Department of Physics, Fudan University, Shanghai 200433, People's Republic of China*

[3]*LAboratoire des Sciences et Matériaux pour l'Electronique, et d'Automatique, Clermont Université, CNRS/Université Blaise Pascal, F-63177 Aubière cedex, France*

[4]*A. M. Prokhorov General Physics Institute, Russian Academy of Science, 119991 Moscow, Russia*

(Received 15 September 2010; published 19 January 2011)

Single ZnO microwires are investigated by angle-resolved photoluminescence spectroscopy. We show that confined optical modes similar to whispering gallery modes can strongly interact with excitons to form one-dimensional exciton polaritons at room temperature, with normal mode splitting exceeding 200 meV. With such a splitting, which is much larger than LO phonon energy, a strong quenching of the polariton-phonon interaction is achieved, even at room temperature and for large excitonic fractions. Thus, a record figure of merit of 50 for the ratio of the Rabi splitting to the polariton full width at half maximum is achieved as a consequence of negligible thermal contribution to dephasing.

DOI: 10.1103/PhysRevB.83.041302 PACS number(s): 78.67.Lt, 71.36.+c, 78.55.Et, 78.66.Hf

Exciton polaritons (polaritons) are bosonic quasiparticles resulting from the strong coupling between excitons (electron-hole pairs bound by Coulomb interaction in semiconductors) and electromagnetic-field waves in bulk semiconductors[1] or in photonic heterostructures such as Fabry-Pérot microcavities.[2,3] In recent years, microcavity polaritons have attracted increasing interest owing to unique physical properties, e.g., an effective mass lighter than that of free electrons by four orders of magnitude.[3] This is the key parameter that permitted polaritons to undergo Bose-Einstein condensation at 20 K.[4] This critical temperature is actually limited by the polariton stability against higher density and temperature, which directly depends on the exciton binding energy and the strength of light-matter interactions. Thus, intense efforts have been carried out over the past decade to realize photonic structures by using wide band-gap semiconductor materials such as III-nitrides or zinc oxide, which offer both large exciton oscillator strength and binding energy (25 and 60 meV binding energy, respectively). However, the epitaxial growth of photonic devices of high structural quality is challenging with these materials, owing to the lack of adapted substrates and a large lattice mismatch within the same family of materials: For example, nitride materials suffer from a 4% lattice mismatch between GaN and AlN and from a −10% lattice mismatch between GaN and InN. Nevertheless, the strong coupling regime has been achieved at room temperature in advanced planar GaN and ZnO microcavities,[5–8] and a convincing indication of polariton lasing has been obtained in a nitride-based planar microcavity.[6] In all these photonic structures, the Rabi splitting is typically 50–60 meV at room temperature, and the figure of merit is 4 at best, limited by both the microcavity structural quality and the large phonon damping.

Following a recent work on ZnO,[9] we chose a different strategy to achieve the strong coupling regime at room temperature. Single-crystalline (Wurtzite) ZnO microwires of hexagonal cross section, with a typical length of 50 μm and a diameter of 1 μm, are grown by a vapor-phase transport method under atmospheric pressure at ∼900 °C.[10] Wurtzite *C*-axis is found to coincide with the wire main axis. Surprisingly, this rather simple growth method provides excellent regularity of the hexagonal shape and very low surface roughness, as shown by the scanning electron microscope (SEM) image of the microwire used in this work in Fig. 1(b). Thus high-quality hexagonal-cavity whispering gallery modes (HWGMs) are sustained in the microwires without any additional technological processing: Quality factors of 800 are reported in this work for modes close to the excitonic transition energy. These modes are strongly coupled with the free bulk excitons lying at ∼3.30 eV (*A*, *B*, and *C* exciton states) at room temperature.[11] A Rabi splitting as large as 280 meV was reported already in Ref. 9 in a similar structure.

To obtain a deeper insight on the intrinsic properties of this kind of polariton, we have performed space- and angle-resolved photoluminescence (PL) spectroscopy of single ZnO microwires at various temperatures (5–300 K). The luminescence, excited by the 325-nm line of a He-Cd laser, is collected by a 0.5 numerical aperture (NA) objective. The luminescence image or its Fourier transform (Fourier plane) can be projected onto the entrance slit of a monochromator, providing, respectively, spectrally resolved microphotoluminescence or a direct access to the (momentum, energy) dispersion of polaritons along the slit direction. Importantly, this procedure provides access to the homogeneous linewidth of polaritons for any given momentum, and provides a reliable estimation of the Rabi splitting.

Angle-resolved PL obtained at room temperature on microwire 1 are shown in Figs. 2(a) and 2(b) for two different orientations of the detection angles θ and ϕ, respectively (see Fig. 1). Owing to the translational invariance along the wire main axis *z*//*C*, the emission angle θ shown in Fig. 2(a) is related to the polariton scalar momentum by $k_z = E\ \sin(\theta)/\hbar c$. Thus Fig. 2(a) represents the dispersion of polaritons in the (momentum k_z, energy) plane. Several well-defined lower polariton branches are visible, which can be separated into two families according to their linear polarization, i.e., mostly TE with respect to the main axis of the wire (electric field *E* perpendicular to the wire *C*-axis, right-hand side of the figure) or mostly TM (*E*//*C*, left-hand side) at $k_z = 0$ ($\theta = 0$). These two polariton families result from the two linearly cross-polarized exciton families

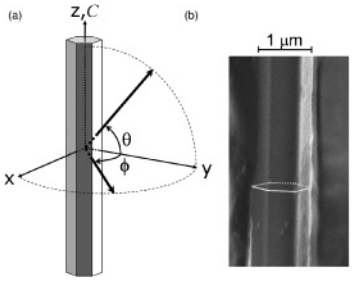

FIG. 1. (a) Definition of the angles θ and ϕ as used in the text. (b) SEM image of the microwire under study. The measured radius is 500 ± 20 nm. The gray solid and dashed line materializes the microwire hexagonal cross section.

found in ZnO, i.e., *A* and *B* are TE-polarized excitons, while *C* are TM-polarized excitons. Within a given polarization family, several lower polariton branches are visible, stacked one over the other in energy. Each branch results from the strong coupling between free excitons and a given HWGM mode (the corresponding label of the HWGM is shown in Fig. 2). Their dispersion features demonstrate unambiguously the strong exciton-photon coupling regime: (i) Modes of high energy (i.e., closer to the exciton resonances) have a dispersion shape that tends to flatness, while those at lower energy are markedly dispersed; (ii) an inflexion point shows up at $\theta \sim 40°$–$50°$, which results from the onset of anticrossing between the involved HWGM and the exciton level.

Given the numerous excitonic and photonic levels involved in this system, we turned to a semiclassical calculation to draw a theoretical description of these polaritons. The Maxwell equations are solved inside and outside the wire assuming infinite length and a cylindrical cross section. The k_z dependence is explicitly taken into account. An anisotropic dielectric function,

$$\varepsilon_{r(z)}(\omega) = \varepsilon_\infty \left(1 + \sum_{t=A,B,C} \frac{\omega_{t,\mathrm{LT}}^{r(z)}}{\omega_{t,\mathrm{ex}} - \omega - i\gamma}\right),$$

is used inside the wire to describe the response of the main bright excitonic transitions to an optical field of frequency ω. ε_∞ is the background dielectric function, $\omega_{t,\mathrm{LT}}$ is the longitudinal-transverse splitting associated with each transition, $\hbar\omega_t$ is the excitonic transition energy, and γ is the nonradiative exciton linewidth (details are published in Ref. 12). The results regarding the various branches and their dispersion [Fig. 2(a), dashed-dotted lines] and polarization (not shown) are in excellent agreement with the measurements. Depending on the mode label, normal mode Rabi splittings ranging from 170 to 200 meV are deduced from this calculation and fit well with temperature-resolved measurements (not shown). This value, smaller than that expected in bulk ZnO (∼300 meV) (Ref. 13), results from the evanescent part of the HWGM modes, which obviously does not overlap excitons. This evanescent field is even larger in the case of a hexagonal cross section (more lossy) as compared to the case of a circular cross section. To this should be added the nonperfectly homogeneous exciton spatial distribution in the material, in particular, in the vicinity of the semiconductor-air interfaces where a large electric field can be found.[14]

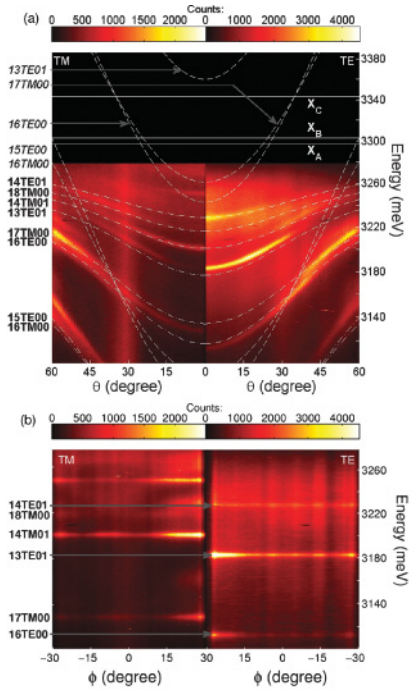

FIG. 2. (Color online) Angle-resolved and polarization-resolved (right: TE; left: TM) room-temperature PL of microwire 1 (microwire with constant diameter). The emission intensity is color scaled and increases from black to yellow (black to white). (a) Angle θ resolution. The white dashed lines are the calculated dispersion of uncoupled HWGM modes. The white dashed-dotted lines represent the calculated exciton-polariton modes. (b) Angle ϕ resolution. The labels "*mPn*" on the left-hand side of the figure refer to the polariton mode quantum numbers (azimuthal *m*, and radial *n*) and polarization (P = TE or TM) according to the HWGM they derive from (calculated HWGM modes have their labels in italics).

Figure 2(b) shows the measured polariton dispersion versus the angle ϕ. Polariton modes are now found to be strictly dispersionless, i.e., strictly monomode in the plane perpendicular to the wire main axis. This is a direct evidence of the one-dimensional (1D) nature of the polaritons investigated here, rarely achieved before and, to the best of our knowledge, never with such a figure of merit at room temperature. For instance, in Ref. 15 and more recently in Ref. 16, a 1D confinement of exciton polaritons was achieved at low temperature (5 K) in arsenide-based microcavities etched into waveguides. In Ref. 17 polariton resonances are reported at room temperature in ZnO nanowires. However, in this experiment, the wires have a small diameter (200 nm) and a short length (a few micrometers), such that exciton polaritons are instead confined longitudinally by both cleaved ends of the wire.

The second important result of this Rapid Communication is the spectral sharpness of the polariton emission as shown in Fig. 2. A measured FWHM of only 4 meV is found (mode 13TE01) for polaritons with 40% excitonic fraction (zero exciton-photon detuning), leading to a record figure of merit of 50 for the strong coupling regime at room temperature. At first glance, this small linewidth seems to be contradictory to the phonon-induced linewidth of 40 meV reported for bare excitons at room temperature in ZnO thin layers.[18] Indeed, the simplest model to account for the polariton linewidth is that of two damped harmonic oscillators coupled together. In this

limit the polariton linewidth scales as the mean value of the bare exciton linewidth (owing to exciton-phonon scattering) and the photon linewidth (owing to photon escape). However, as explained in Ref. 19, when the phonon contribution to the polariton linewidth (thermal contribution) needs to be considered, this crude assumption is, in general, incorrect because the exciton-photon interaction dominates over the exciton phonon by one order of magnitude. Then, the correct physical picture to explain the thermal contribution to the polariton linewidth is scattering between polaritons and phonons. Low-temperature experiments with microcavities have shown already that this mechanism was leading to a significant reduction of polariton scattering with acoustic phonons.[20,21] In the present work, this effect is even more pronounced in spite of the fact that it is observed at room temperature where scattering with the thermal population of optical phonons cannot be neglected. To get a better understanding of this effect, we use the Fermi "golden rule" to compute the 1D polariton scattering rate Γ with acoustic and optical phonons.[22] An important assumption can be made: Because the polariton density of states is four orders of magnitude lower than that of bare excitons, the scattering rate from one polariton branch to another one can be neglected as compared to the scattering of polaritons toward bare excitons. In this limit, the scattering rate of polaritons of energy E_{LP} with thermal phonons reads

$$\Gamma(E_{\mathrm{LP}}) = \pi V X(E_{\mathrm{LP}}) \int d^3\mathbf{q}(2\pi)^{-3} N(\mathbf{q}) \times [|M_{\mathrm{ac}}(\mathbf{q})|^2 \delta(E_{\mathrm{LP}} - E_X(\mathbf{q}) + E_{\mathrm{ac}}(\mathbf{q})) + |M_{\mathrm{LO}}(\mathbf{q})|^2 \delta(E_{\mathrm{LP}} - E_X(\mathbf{q}) + E_{\mathrm{LO}})].$$

$X(E_{\mathrm{LP}})$ is the excitonic fraction of the considered polariton state, V is a quantization volume, $\mathbf{q}$, $E_{\mathrm{ph}}(\mathbf{q})$ and E_{LO} are the phonon momentum and energies, respectively, and $M_{\mathrm{ac\,(LO)}}(\mathbf{q})$ are the matrix element for exciton and acoustic phonon (optical LO phonon) interaction. The polariton momentum is negligible as compared to $\mathbf{q}$. The phonons are assumed to be at thermal equilibrium, thus following a Bose distribution $N(\mathbf{q})$ at the lattice temperature. The results of this calculation are shown in Figs. 3(a) and 3(b) as red solid lines for temperatures of 70 K [Fig. 3(a)] and 300 K [Fig. 3(b)], respectively.

At low temperature, only low-energy acoustic phonons are populated, and the LO-phonon population has vanished. Therefore the polariton-phonon scattering only induces a low thermal broadening over the whole range of lower polariton energy [the red plot in Fig. 3(a)]. At room temperature, thermal broadening increases dramatically, but only for polariton modes contained within the energy range $\Delta = (E_X, E_X - E_{\mathrm{LO}})$ ($E_{\mathrm{LO}} = 72$ meV), while those at lower energy remain virtually unaffected regardless of their excitonic fraction [the red plot in Fig. 3(b)]. The reason is as follows: At room temperature, polaritons where energy is contained within Δ can undergo scattering with a thermal LO phonon and end up in the pure excitonic states of large momentum. This is a very efficient process because of the large exciton–LO-phonon matrix elements and because of the very high density of states of pure exciton states. A second kink is visible on this plot [Fig. 3(b), red plot at ~3290 meV], which is owing to the contribution of acoustic phonons in this energy range. For polariton states of energy lower than Δ, LO-phonon (and *a fortiori* acoustic-phonon) energy is too low to scatter a polariton to the pure exciton states of large momentum. Instead, the scattering can end up only in the polariton states, a process strongly weakened as compared to the previous one owing to the very low density of polariton states.

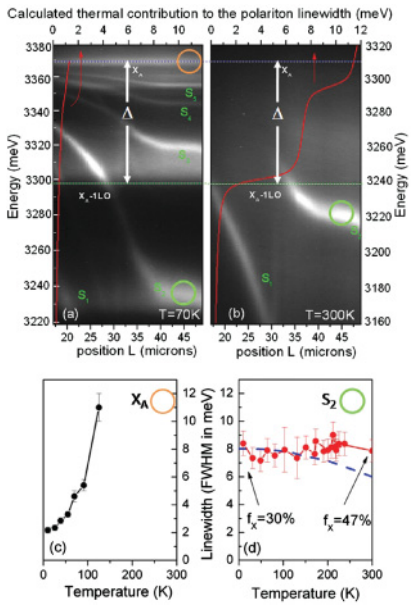

FIG. 3. (Color online) Spatially resolved TE-polarized emission spectrum along a 32-μm segment of microwire 2 (tapered microwire) at temperature (a) $T = 70$ K and (b) $T = 300$ K. Along this portion of the microwire, the inhomogeneous diameter (presently increasing from left to right) provides a natural way to continuously vary the exciton-photon detuning. S_1–S_5 label the five visible polariton modes at 70 K. The $\Delta = (E_X, E_X - E_{\mathrm{LO}})$ energy range is shown by the white arrows. Red (dark gray) solid lines show the calculation of the phonon contribution to the polariton linewidth vs energy. (c) Pure exciton linewidth vs temperature [energy and position shown by the orange (gray) circle in (a)]. (d) Measured homogeneous linewidth of polariton mode S2 vs temperature [red (dark gray) round symbols], when its energy lies below Δ. The dashed blue (black) line plots the photon-escape contribution to the linewidth (100% contribution to the linewidth at 10 K). The homogeneous linewidths are obtained from angle-resolved measurement carried out in a region centered on $L = 43$ μm [green (light gray) circles in (a) and (b)].

We have verified this effect experimentally. To do so, we have analyzed the temperature dependence of polariton emission in a tapered microwire (microwire 2). This tapered shape allows tuning of the polariton energies along the wire axis, as discussed in Ref. 9. The results are shown Fig. 3. The black-and-white images in Figs. 3(a) and 3(b) are the PL intensity plots (gray scale) obtained at 70 and 300 K, respectively, with spatial resolution (x axis) and spectral resolution (y axis), of a segment of microwire 30 μm long. At 70 K, sharp polariton modes are visible within the energy range Δ (modes S3, S4, and S5) as well as below Δ (modes S1 and S2). Their curved shape is owing to the tapered shape of the microwire: The diameter increases from left to right. At 300 K, however, polariton modes S3, S4, and S5 as well as the part of the S2 mode where energy falls within Δ (corresponding to positions $L < 34$ μm along the wire axis) are completely washed out by phonon damping [Fig. 3(b)]. On the other hand, the part of the S2 mode where energy is lower than

Δ (positions $L > 34$ μm) remains unaffected, showing that phonon damping is strongly suppressed below Δ.

A more direct and quantitative demonstration of this effect is obtained by performing a measurement of the polariton linewidth versus temperature. To do so, a polariton mode of energy situated directly below Δ [mode S2 at $L = 40$ μm, green circle in Fig. 3(a)] is chosen. For the sake of comparison, the linewidth of free exciton A is also measured [same position, $L = 40$ μm, white circle in Fig. 3(a)]. The results are shown Figs. 3(c) and 3(d). For temperatures increasing from 10 to 300 K, the linewidth of polariton mode S2 linewidth stays fixed at 8 meV. At 10 K, this value corresponds uniquely to the HWGM damping contribution. Upon increasing temperature, this contribution decreases slightly owing to the change of excitonic fraction (30%–47%), and can be calculated. It is shown by the blue dashed plot of Fig. 3(d). Thus, the thermal contribution to the polariton linewidth is the difference between the dashed blue plot and the total linewidth (red plot): It does not exceed 3 meV at 300 K. This result is particularly striking when one considers the excitonic fraction of this mode, 47% at 300 K. For comparison, the thermal contribution to the bare exciton linewidth [Fig. 3(c)] amounts to 9 meV, already at 120 K [Fig. 3(c)]. It becomes too broad at larger temperatures to be measured properly.

From these considerations, a general criterion can be drawn for a polariton with 50% excitonic fraction to be preserved from thermal phonon damping: Half of the normal mode splitting must exceed the LO phonon energy, i.e.,

$$\hbar\Omega/2 > E_{\mathrm{LO}}.$$

In practice, this criterion is, in general, difficult to meet, considering the large LO phonon energy in most semiconductors as compared to the Rabi splitting usually achieved in microcavities. In this Rapid Communication, we have shown that with ZnO microwires this criterion is met, thanks to the very large oscillator strength combined with the microwire geometry that provides a large Rabi splitting.

In this Rapid Communication, we have shown that the strong coupling between whispering gallery modes and excitons in ZnO microwires results in the formation of 1D exciton polaritons, with record Rabi splitting of ~200 meV. We demonstrated experimentally and theoretically that these 1D polaritons can be thermodynamically decoupled from the phonon bath, a very advantageous situation to maintain high coherence at elevated temperatures. Thus, with a record exciton binding energy of 60 meV, polaritons in ZnO microwires appear as one of the most promising Bose gases for fundamental physics and practical applications. For example, by adjusting the photon-exciton detuning with the wire diameter, one can change the strength of the repulsive polariton interaction to address the various 1D physics issues, e.g., quantum fluctuations and quasicondensation,[23] thermalization and quantum Newton's cradle,[24] fermionization in a Tonks-Girardeau gas,[25] etc. The demonstration of high-quality polaritons in ZnO microwires also opens prospects for the fabrication, in the near future, of ultracompact and low-cost polariton "lasers,"[26] ultrafast parametric amplifiers,[27] or nonclassical sources of photon pairs[28] operating at unprecedented high temperatures.

ACKNOWLEDGMENTS

A.T., M.R., and L.S.D. acknowledge support of the French Nanoscience foundation (Project No. FCSN-2008-10JE "RICOPHIN"). G.M. acknowledges support of the FP7 ITN Spin-Optronics (No. 237252). L.S., W.X., and Z.C. acknowledge financial support from the NSFC (No. 10874031) and "973" project of the Ministry of Science and Technology of China (No. 2011CB925602)

[1] J. J. Hopfield, Phys. Rev. **112**, 1555 (1958).
[2] C. Weisbuch, M. Nishioka, A. Ishikawa, and Y. Arakawa, Phys. Rev. Lett. **69**, 3314 (1992).
[3] A. Kavokin and G. Malpuech, *Cavity Polaritons* (Elsevier Academic Press, Amsterdam, 2003).
[4] J. Kasprzak *et al.*, Nature (London) **443**, 409 (2006).
[5] G. Christmann *et al.*, Phys. Rev. B **77**, 085310 (2008).
[6] G. Christmann, R. Butte, E. Feltin, J.-F. Carlin, and N. Grandjean, Appl. Phys. Lett. **93**, 051102 (2008).
[7] R. Shimada, J. Xie, V. Avrutin, U. Ozgur, and H. Morkoç, Appl. Phys. Lett. **92**, 011127 (2008).
[8] J.-R. Chen *et al.*, Appl. Phys. Lett. **94**, 061103 (2009).
[9] L. Sun *et al.*, Phys. Rev. Lett. **100**, 156403 (2008).
[10] Y. Ke *et al.*, Mater. Lett. **59**, 1866 (2005).
[11] C. Klingshirn *et al.*, Adv. Solid State Phys. **45**, 275 (2006); B. Gil, Phys. Rev. B **64**, 201310 (2001).
[12] G. Pavlovic, G. Malpuech, and N. A. Gippius, Phys. Rev. B **82**, 195328 (2010).
[13] M. A. Kaliteevski, S. Brand, R. A. Abram, A. Kavokin, and L. S. Dang, Phys. Rev. B **75**, 233309 (2007).
[14] C. Soci *et al.*, Nano Lett. **7**, 1003 (2007).
[15] G. Dasbach, M. Schwab, M. Bayer, D. N. Krizhanovskii, and A. Forchel, Phys. Rev. B **66**, 201201(R) (2002).
[16] E. Wertz *et al.*, Nature Phys. **6**, 860 (2010).
[17] L. K. van Vugt, S. Ruhle, P. Ravindran, H. C. Gerritsen, L. Kuipers, and D. Vanmaekelbergh, Phys. Rev. Lett. **97**, 147401 (2006).
[18] C. Klingshirn, R. Hauschild, J. Fallert, and H. Kalt, Phys. Rev. B **75**, 115203 (2007).
[19] V. Savona and C. Piermarocchi, Phys. Status Solidi A **164**, 45 (1997).
[20] J. J. Baumberg, A. Armitage, M. S. Skolnick, and J. S. Roberts, Phys. Rev. Lett. **81**, 661 (1998).
[21] P. Borri, J. R. Jensen, W. Langbein, and J. M. Hvam, Phys. Rev. B **61**, R13377 (2000).
[22] S. Rudin, T. L. Reinecke, and B. Segall, Phys. Rev. B **42**, 11218 (1990).
[23] S. Richard, F. Gerbier, J. H. Thywissen, M. Hugbart, P. Bouyer, and A. Aspect, Phys. Rev. Lett. **91**, 010405 (2003).
[24] T. Kinoshita, T. Wenger, and D. S. Weiss, Nature (London) **440**, 900 (2006).
[25] B. Paredes *et al.*, Nature (London) **429**, 277 (2004).
[26] M. Zamfirescu, A. Kavokin, B. Gil, G. Malpuech, and M. Kaliteevski, Phys. Rev. B **65**, 161205 (2002).
[27] M. Saba *et al.*, Nature (London) **414**, 731 (2001).
[28] C. Ciuti, Phys. Rev. B **69**, 245304 (2004).